

# The structure of an *in-situ* formed titanium-boron-carbon coating on a graphite substrate

Jin-hua Yang<sup>1,2</sup>, Quan-gui Guo<sup>2</sup>, Zhan-jun Liu<sup>2,\*</sup>, Hai-peng Qiu<sup>1</sup>, Jian Jiao<sup>1</sup>

1. AVIC Composite Corporation LTD, Beijing 101300, China

2. Key Laboratory of Carbon Materials, Institute of Coal Chemistry, Chinese Academy of Sciences, Taiyuan 030001, China

**Abstract:** A titanium-boron-carbon coating was fabricated on a graphite substrate by heating TiB<sub>2</sub> powder on a graphite surface above the eutectic temperature. The coating consisted of a pure graphite layer on the outer surface and a TiB<sub>2</sub>-C alloy layer inside. The graphite layer had many wrinkles due to the difference in the thermal expansion coefficients of TiB<sub>2</sub> and graphite. The TiB<sub>2</sub>-C alloy layer had a continuous three-dimensional interpenetrating network microstructure. The  $d_{002}$  value of the graphite in the alloy layer was 0.335 6 nm, which was quite close to that of single crystal graphite (0.335 4 nm). Raman and X-ray photoelectron spectroscopy indicated that the graphite in both layers was doped substitutionally with boron atoms. A water quench thermal shock test verified a high adhesion strength between the coating and the substrate. This method is promising for the fabrication of thermal barrier coatings on carbon materials.

**Keywords:** Colloidal silica; Sucrose; Graphene; Anode; Li-ion batteries

## 1. Introduction

Graphite and carbon fiber reinforced materials are widely used in the aerospace and aviation fields such as nose tips and rocket nozzles owing to their advantages such as low density, high thermal conductivity and high strength at high temperatures<sup>[1-4]</sup>. However, these carbon materials have a fatal drawback that they are easily oxidized above 673 K<sup>[5]</sup>. On the other hand, ultra-high temperature ceramics such as some borides (TiB<sub>2</sub>, ZrB<sub>2</sub>, HfB<sub>2</sub>, et al.) and carbides (TiC, ZrC, HfC, et al.) have drawn much attention because they can withstand hostile and reactive environment<sup>[6,7]</sup>. Therefore, it is reasonable to combine these two kinds of materials together to make full use of their advantages, and two common methods to combine them are coating ceramics on carbon materials<sup>[8-10]</sup> or adding ceramics into carbon materials<sup>[11-16]</sup>.

Many researchers have found that adding titanium boride (TiB<sub>2</sub>) into carbon materials could effectively improve their oxidation resistance<sup>[17, 18]</sup>. However, in the real application fields, coating is preferred since it will not change the properties of the base materials. From phase diagram and others' work, we know that TiB<sub>2</sub> and carbon could form eutectic<sup>[19, 20]</sup>. So, it will be a promising way to fabricate thermal barrier coating *in-situ* on carbon materials using an eutectic method. In the present work, we heated TiB<sub>2</sub> powder and graphite above their eutectic temperature to make a thermal barrier coating, and the structure of the coating was studied.

## 2 Experimental

Firstly, high-purity graphite cuboid plates (99.95 wt.%), with a bulk density of 1.74 g/cm<sup>3</sup>, porosity of 14.2 % and the pore size distribution shown in , were machined into a dimension of 50×50×5 mm. The surface of these graphite plates was ground with 2000-grit SiC grinding paper followed by cleaning with acetone, alcohol, and distilled water in sequence in an ultrasonic cleaner and then dried. Secondly, 1.5 g of TiB<sub>2</sub> powder (<200 mesh, 99.95 wt.%, General Research Institute for Nonferrous Metals, Beijing) was piled up on the top of graphite plate into the square shape of 30×30 mm. The sample was then heated to 2823 K in a graphitization furnace with a heating rate of about 20 K/min without maintaining time, under a purified Ar atmosphere. A control sample without TiB<sub>2</sub> powder was also prepared with the same procedure. After the heat-treatment, the graphite plate heated with TiB<sub>2</sub> powder was broken into two halves: one half was used to see the fracture-surface microstructure and the other half was ground with 2000-grit SiC grinding paper to see the distribution of the phases. Moreover, TiB<sub>2</sub> phase was removed by immersing the sample in a boiling NaOH water solution (30 wt. %, boiling point 119 °C) for 5 h to see the distribution of the TiC phase. The microstructure was observed by a field emission scanning electron microscope (SEM; JSM-7001F, JEOL), and using an energy dispersive spectrometer, precise

Received date: 05 May 2017; Revised date: 30 Sep 2017

\*Corresponding author. E-mail: zjliu03@sxicc.ac.cn

Copyright©2017, Institute of Coal Chemistry, Chinese Academy of Sciences. Published by Elsevier Limited. All rights reserved.

DOI: 10.1016/S1872-5805(17)60135-5

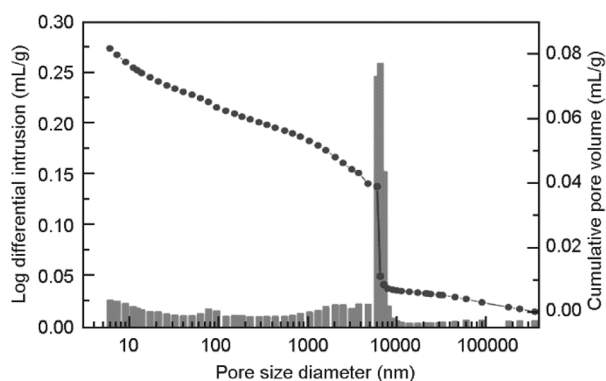


Fig. 1 Distribution of pore size of the graphite plate.

elemental composition of materials with a high spatial resolution was obtained. The optical microscopy was characterized by using a metallographic microscope (MV6000, PR China) to see the upper-surface microstructure of the coating. A X-ray diffractometer (XRD; D8 Advance, Bruker) with Cu  $K\alpha$  radiation ( $\lambda = 0.15406$  nm, 40 kV and 40 mA) was used to determine the phases and parameters of the graphite crystal,  $d_{002}$  and  $L_c$ , where  $d_{002}$  and  $L_c$  were the graphite interlayer distance and the apparent crystallite thickness, respectively [21]. The samples were crushed into powders to remove the stresses formed inside [22, 23], and silicon powder was added as an internal standard to calibrate the shifting of diffraction profiles. The value of  $d_{002}$  was calculated using the Bragg's law,  $d_{002} = \lambda / (2\sin\theta)$ , where  $\theta$  was the scattering angle,  $\lambda$  was the wave length of the X-ray, and the  $L_c$  was calculated by the Scherrer's formula  $L = K\lambda / (\beta\cos\theta)$ , where  $\beta$  was the full width at half maximum intensity (FWHM). The form factor  $K$  was 1 for  $L_c$  [21].

The Raman scattering spectra excited by the 532.25 nm radiation were obtained with a Raman spectrometer (Jobin Yvon, Labram HR 800, 1 mW) in the 1000-3500  $\text{cm}^{-1}$  range at room temperature. The chemical bonding was analyzed using X-ray photoelectron spectroscopy (XPS; Axis Ultra DLD, Kratos, 1486.6 eV Al- $K\alpha$  radiation).

### 3 Results and discussion

TiB<sub>2</sub>-C coating (Fig. 2a) was formed in-situ on the surface of the graphite plate after heat treatment at 2823 K, which was above the eutectic temperature of TiB<sub>2</sub>-C system (2780 K, 32 mol. % C) [20]. As shown in Fig. 2b, the coating had very bright surface which was smooth enough to be observed directly using an optical microscope. As can be seen, the surface has smooth areas separated from each other by many wrinkles which are indicated by the arrows in Fig. 2b and c. Backscattered electron imaging in scanning electron microscopy has led to possibilities for the evaluation of phase distribution on a microscopic level [24]. The uniform grey-levels seen in Fig. 2d indicate that only one phase exists on the surface of the coating. X-ray mapping and the corresponding spectra (Fig. 2e and f) show that only carbon element is detected. Since the solubility of carbon in the

TiB<sub>2</sub>-C melt decreased with the decrease of the temperature, during the cooling process, the excess carbon crystallized on the surface of the coating. The formation mechanism of graphite wrinkles is believed to be due to the thermal expansion coefficient difference between TiB<sub>2</sub> and graphite [25-29]. In our case, the thermal expansion of TiB<sub>2</sub> varies from 7.4 to  $9.8 \times 10^{-6} \text{ K}^{-1}$  for the temperature range from 293 to 2273 K (extrapolate to 2773 K:  $10.34 \times 10^{-6} \text{ K}^{-1}$ ) [30], while the in-plane thermal expansion coefficient of graphite changes from  $-1.25$  to  $1.50 \times 10^{-6} \text{ K}^{-1}$  for the same temperature range [31]. During the solidification process, a compressive biaxial stress developed on the graphite layer, leading to the formation of triangular folds on the surface [29].

In order to study the inside structure of the coating, the sample was fractured into two halves. The fractured coating with a thickness of about 2 mm in the center was shown in Fig. 3a, and the corresponding backscattered electron image was shown in Fig. 3b. As shown by the yellow arrows, large-scale graphite layers are found, which indicate that the fracture mainly happens parallel to the basal-plane direction of graphite. The inset in Fig. 3a and the inset in Fig. 3b show the cross section of one graphite layer which is less than 10  $\mu\text{m}$  thick, and the layered structure of graphite can be clearly seen. The morphology of the fracture surface after being ground is shown in Fig. 3c and 3d, from which we can see the distribution of the phases. It can be seen that the coating inside has a continuous three-dimensional interpenetrating microstructure as observed in many ceramic oxides [32]. Since TiB<sub>2</sub> and TiC phases have the same contrast ratio in backscattered electron images, TiB<sub>2</sub> was removed from the alloy using a boiling NaOH solution in order to distinguish the distribution of TiC and TiB<sub>2</sub>. After the removal of TiB<sub>2</sub> phase, almost only graphite is left with trace amount of TiC depicted by the red arrows in Fig. 3e and 3f, which indicate that the alloy is mainly composed of TiB<sub>2</sub> and graphite with a trace amount of TiC. The conjunction area between the coating and graphite substrate is shown in Fig. 3g and 3h. As indicated by the arrows in Fig. 3h, lots of small size TiB<sub>2</sub>/TiC particles distributed inside the conjunction area. When the eutectic was in liquid form at high temperatures, the liquid entered into the holes due to the capillary effect. The conjunction area does good to the adhesion strength between the coating and the substrate.

To further study the structure of graphite formed in the coating, XRD, Raman and XPS analysis were employed. From XRD patterns (Fig. 4a) we can know that the coating is mainly composed of TiB<sub>2</sub> and graphite with a little amount of TiC, which is in agreement with SEM analysis. Table 1 indicates that the  $d_{002}$  value of the graphite in the coating is 0.3356 nm, which is quite close to that of single crystal graphite (0.3354 nm). Since we used the powder diffraction method, the stresses should not be large enough to influence the results [22, 23], and the slight shift in lattice parameter may be due to B-doping of the graphite as well as the not fully released stress effect [32, 33].

Download English Version:

<https://daneshyari.com/en/article/7954216>

Download Persian Version:

<https://daneshyari.com/article/7954216>

[Daneshyari.com](https://daneshyari.com)